ASM Sci. J.Special Issue 2018(1) AiMS2018, 8-16

The Effect of Sm_2O_3 Nanoparticle Inclusion on Superconducting Properties of YBCO Ceramics

R. Aima[1*], S. A. Halim[2], S. K. Chen[2] and M. M. Awang Kechik[2]

[1] *Advanced Nano Materials (ANoMa) Research Group,*
School of Fundamental Science, Universiti Malaysia Terengganu,
21030 Kuala Nerus, Terengganu, Malaysia.

[2] *Superconductivity and Thin Film Laboratory, Department of Physics,*
Universiti Putra Malaysia, 43400 Serdang, Selangor, Malaysia.

Polycrystalline samples of $YBa_2Cu_3O_{7-\delta}$ added with small amounts (x = 0.0 - 1.0 wt%) of Sm2O3 nanoparticles were synthesized via co-precipitation process. The effects of addition of Sm_2O_3 nanoparticles on the superconducting properties and crystal structure of $YBa_2Cu_3O_{7-\delta}$ were thoroughly elucidated. The superconducting transition temperature *(T_c)* of each sample was measured by a standard four point probe method. As the addition of nano-Sm_2O_3 increases, the reduction of T_c occur from 92 K for x = 0.0 to 80 K for x = 1.0 wt% attributable to oxygen vacancy disorder. The crystal lattice parameters of all samples were determined by X-ray diffraction (XRD) with the Rietveld refinement technique. It was found that the samples are predominantly single phase perovskite structure Y-123 with orthorhombic, small amount of Y-211 and unreacted Sm_2O_3 secondary phases for samples x = 0.2 - 1.0 wt%. Besides, the structure from SEM images showed that the structure becomes more porous than the pure sample and the grain sizes are getting slightly decrease as the addition of Sm_2O_3 nanoparticles increase. The addition of nano-Sm_2O_3 disrupts the grain growth of YBCO (123), therefore resulting in the degradation of microstructure and superconducting properties of the samples.

Keywords: YBCO, superconducting transition temperature, co-precipitation, nanoparticles

I. INTRODUCTION

High temperature superconductor (HTS) in the copper based were discovered by J. G. Bednorz and K. A. Muller in 1986 resulted in worldwide interest in these materials [1]. $YBa_2Cu_3O_{7-\delta}$ (Y123) is one of the most important copper oxide based superconductors that has received great attention since it was revealed by Wu in 1987 [2]. Y123 has significance advantages such as high current density, J_c, high critical temperature, T_c, excellent capabilities of trapping magnetic fields, and better mechanical properties; for which the enhancement of these properties is the key of superconductors technology application [3].

*Corresponding author:aima.ramli@umt.edu.my

However, since Y123 superconductor is granular in nature, it contributes to weak grain boundary connections, poor flux pinning and inhomogeneity in the bulk samples. Thus, resulting in low T_c and J_c in the presence of magnetic field. Therefore, to improve the homogeneity and weak links effect, co precipitation method is chosen due to low reaction temperature, fine and uniform particle size, closely packed with little porosity, easy set-up, economical and time saving processing [4]. Besides, the inclusion of rare earth nanoparticles into Y123 system improves its current carrying capability because the size of nanoparticles is almost similar to magnetic flux diameter of high temperature superconductor [5]. Thus, it may acted as pinning centres that prevent the motion of magnetic flux and increase the J_c. On the other hand, the addition of nano-size particles is expected to change other superconducting properties of Y123, i.e. T_c, due to locally modifying the crystalline structure and generate defects such as twins, tweed, and inhomogeneous micro-defects [6].

It has been reported that by adding magnetic nanoparticles, current carrying capacity of superconductors YBCO was enhanced significantly, such as in the case of Fe3O4 nanoparticle, J_c was about 1683 mA/cm^2 for sample with 0.02 wt%. But, the excessive addition of nano Fe_3O_4 ($> 0.02wt\%$) suppressed the T_c and J_c [7]. Meanwhile, non-superconducting ZrO_2 nanoparticles adding in YBCO serving as artificial pinning centers (APC) cause a remarkable enhancement of critical current density, J_c at 77 K.

The pinning strength of nanoparticles inclusion has been found to be greater with wide size dispersed nanoparticles, 764 nm. This indicates that pinning properties and vortex dynamics depend on the size of artificial pinning centers [8]. Mellekh *et al.*, (2006) worked on YBCO added with small amounts (0 - 0.6 wt%) of alumina particles [9]. Transmission electron microscopy (TEM) and energy dispersive X-ray (EDS) analysis have shown that alumina reacts with the YBCO matrix to form nanometric aluminium-rich inhomogeneities intergrown within the YBCO superconducting matrix. These inhomogeneities reduce the $J_{c-onsett}$ from 91.3 K to 88 K. The reduction of T_c and J_c as the nanosize alumina addition increase due to the counterbalance of two effects; the formation of the nanometric inhomogeneities containing aluminium relevant to the flux pinning and reduction of matrix superconducting volume which reflects the decrease of the critical temperature, $T_c$and critical current density, J_c.

II. EXPERIMENTAL PROCEDURE

A. Samples Preparation

Powder of constituent metal acetates of Yttrium (III) acetate ($Y(CH_3COO)_3.4H_2O$), barium acetate ($Ba(CH_3COO)$) and copper (II) acetate ($Cu(CH_3COO)_2$) with purity $> 99\%$, were weighed in their molar ratio 1:2:3 and dissolved

in acetic acid, namely solution A. Meanwhile, solution B containing 0.5 M oxalic acid was prepared in a mixture of deionized high-purity water : isopropanol (v/v = 1:1.5). Solution B was added drop-wise into solution A in an ice bath with continuous stirring in order to completely dissolve the solutions. A uniform, stable, blue suspension was formed and the slurry was filtered after 5-10 minute of reaction. After filtration, the filtrated cake was allowed to dry at 80 °C overnight. The dried blue precipitates were ground prior to thermal treatment at 900 °C in air for 15 h. The calcined powders were added with nano-Sm_2O_3 (x = 0 - 1.0 wt%) and reground in agate mortar until homogeneous. The mixed powders were pressed into pellets of 13 mm diameter using Specac manually operated hydraulic press. The pellets were sintered at 920 °C for 15 h in air and cooled slowly to room temperature in furnace at a rate 1 °C /min.

B. Characterization and Measurements

The thermal decomposition behaviour of the coprecipitated precursor powders were analysed by using a Mettler Toledo thermobalance (model TGA/SDTA 851e) with a heating rate of 10 °C/min. Samples of approximately 8 g were placed in aluminium pans and heated from 30 °C to 900 °C under a dynamic flow of nitrogen at 50 mL/min. The structure and phase identification of the powder samples ground from sintered pellets were examined by powder XRD using a Philips 1710 diffractometer with Cu Kα radiation. Refinement of the X-ray diffraction data was carried out by the Rietveld method. The surface morphology of the samples was carried out by scanning electron micrograph (SEM). The electrical resistance was measured by using standard four-probe method, in a closed cycle helium cryostat at temperatures between 20 K and 300 K.

III. RESULT AND CHARACTERIZATION

A. Thermo Gravimetric Analysis (TG / DTG)

Figure 1 indicates the thermal decomposition of the YBCO precursor powder during the TG measurement and DTG (derivative of the weight loss curve). From this method, the proper sintering temperature could be estimated [10]. As shown in drop 1 and 2 (<240°C), approximately 19% weight loss is attributed to the dehydration of moisture and water in lattice of the oxalate salts. This dehydration process is also proved by DTG measurements where the drop peaks are in the same temperature range and could be clearly seen. A sharp drop peak is observed in drop 3, approximately 18% weight loss in the temperature range of 250 °C to 356 ° Cas the decomposition of the yttrium oxalate salts to the corresponding carbonates and copper oxalate to corresponding copper oxide.

In drop 4, the decomposition of barium ox-

alate corresponding barium carbonate is observed in the range of temperature 365.7 °C - 568.8 °C respectively. On heating to higher temperature, the composition of barium carbonate to barium oxide takes place at near 760 °C and fully decomposed at 896 °C . At temperature near 900 °C , the formation of YBCO 123 (Y123) phase was produced. However, at temperature above 950 °C , the superconducting YBCO phase is damaged due to oxygen loss and melting. Consequently, from the TG plots, the total losses of mass during the entire thermal decomposition process were found to be 55%.

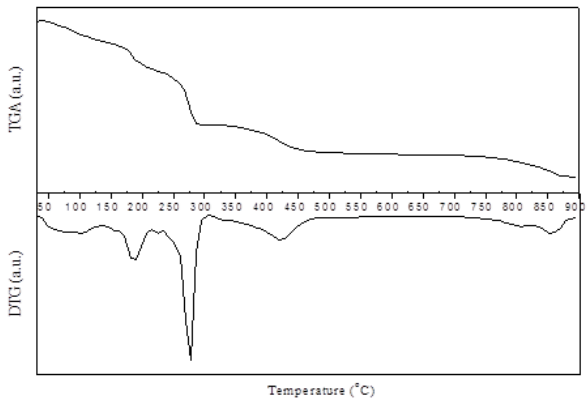

Figure 1. Thermogravimetric (TG/DTG) analysis of the YBCO oxalate powder

and consist of perovskite-like structure Y123 corresponding to orthorhombic *Pmmm* symmetry. The lattice parameters and unit cell volume for pure YBCO sample obtained from the data are a = 3.8211 $\hat{A}$, b = 3.8881 $\hat{A}$, c = 11.690 $\hat{A}$ and V = 173.68 $\hat{A}$. The minor secondary phase, Y-211 and unreacted Sm_2O_3 have been observed for x = 0.2 - 1.0 wt%. This Y211 secondary phase is commonly coexist in YBCO (123) [11]. The lattice parameter, a increased for x = 0.2 - 0.8 wt% but slightly decreased for x = 1.0 wt%. On the other hand, lattice parameter, b decreased and remain almost constant at x = 0.2 - 0.6 wt% and increase slightly at x = 0.8 wt%.

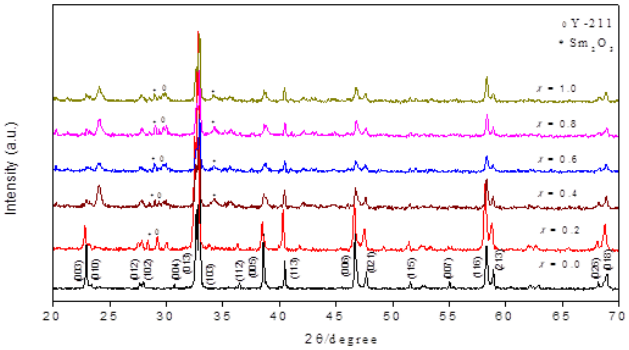

Figure 2. X-ray diffraction pattern of YBCO with various addition of Sm_2O_3

B. X-ray Diffraction (XRD) Pattern

Figure 2 shows the x-ray diffraction patterns of YBCO with addition of various weight percentage of Sm_2O_3. Then these patterns were compared with that of ICDD-PDF-2 database to verify the structural parameters. It showed that the pure sample is dominantly single phase

The lattice parameter c was reducing and remain constant at x = 0.4 - 1.0 wt%, as well. The changing value parameters a as well as b have been lowered the orthorhombicity linearly as plotted in Figure 3. The variation in lattice parameters results from the internal stress induced by Sm inclusion, which Sm3+ has the potential to substitute Y-site due to its ionic radius of Sm3+ (0.964 $\hat{A}$) bigger than Y3+ (0.893$\hat{A}$)

(Veal et al, 1989) [12]. Besides, the oxygen ion may be trapped in the crystal structure and affect the values of lattice constants [2]. All the values of lattice parameters and volume are listed in the Table 1.

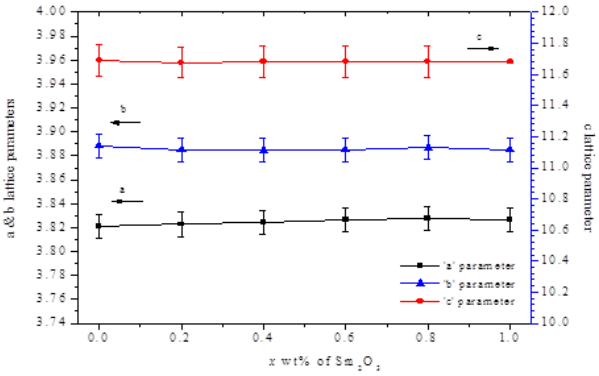

Figure 3. Variation of lattice constants along a-, b- and c- axis for YBCO added with various amounts of Sm_2O_3

C. Microstructure Analysis SEM

The SEM surface morphologies of the YBCO bulk with addition of Sm_2O_3, x = 0.2 - 1.0 wt% were examined and are shown in Figure 4. The average grain sizes of samples were determined from 100 grains with magnification 1000X measured randomly using Image J. As depicted, there are changes in grain size as well as the number of pores. It can be seen the grains in pure sample are strongly linked with less porosity. However, in the case of x = 1.0 wt%, the grains are seem to be molten-like due to the highest amount of Sm_2O_3 adding into YBCO, thus limiting the growth of the crystal structure. The grain size of the samples decreased from 1.880 μm to 1.589 μm as the addition of Sm_2O_3 nanoparticles increased. This is due to the non-homogenous distribution of Sm_2O_3 in structure and poor grain connectivity. The decreasing of grain size also has been reported in the case of SiO_2 nanoparticles, Nd_2O_3 nanoparticles and Au nanoparticles added in YBCO system [13]-[15].

D. Resistance dependence of temperature of YBCO + xSm_2O_3

Figure 5 displays the variation temperature of the normalized resistance of pure sample as well as Sm_2O_3 added samples (x = 0.2, 0.4, 0.6, 0.8 and 1.0). The $T_{c-onset}$ for those samples are 92K, 91K, 90K, 90K, 89K and 88 K, respectively. The pure sample showed metallic behaviour in the normal state. By looking at R-T curves, there is metallic to semiconducting behaviour and double step transition of T_c which is believed due to indication of weak-links behaviour. The samarium added compound shows a T_c slightly lower than that of the pure compound. With increasing Sm_2O_3 content, the transition temperature getting lower, this could be attributed to the suppression of superconductivity by Sm_3+ ions. The transition width, ΔT_c becomes broaden and widens from 4 K to 22 K which indicates the existence of impurities and weak-links between the superconducting grains.

Table 1. Refined unit cell lattice parameters, a, b and c axes and volume fraction percentage for YBCO added with various amounts of Sm_2O_3

x, Sm_2O_3	0.0	0.2	0.4	0.6	0.8	1.0
a ($\hat{A}$)	3.8211	3.8227	3.8239	3.8262	3.8275	3.8267
b ($\hat{A}$)	3.8881	3.8848	3.8846	3.8848	3.8869	3.8852
c ($\hat{A}$)	11.690	11.676	11.683	11.681	11.682	11.682
V ($\hat{A}^3$)	173.6762	173.3982	173.5387	173.6250	173.8003	173.6750

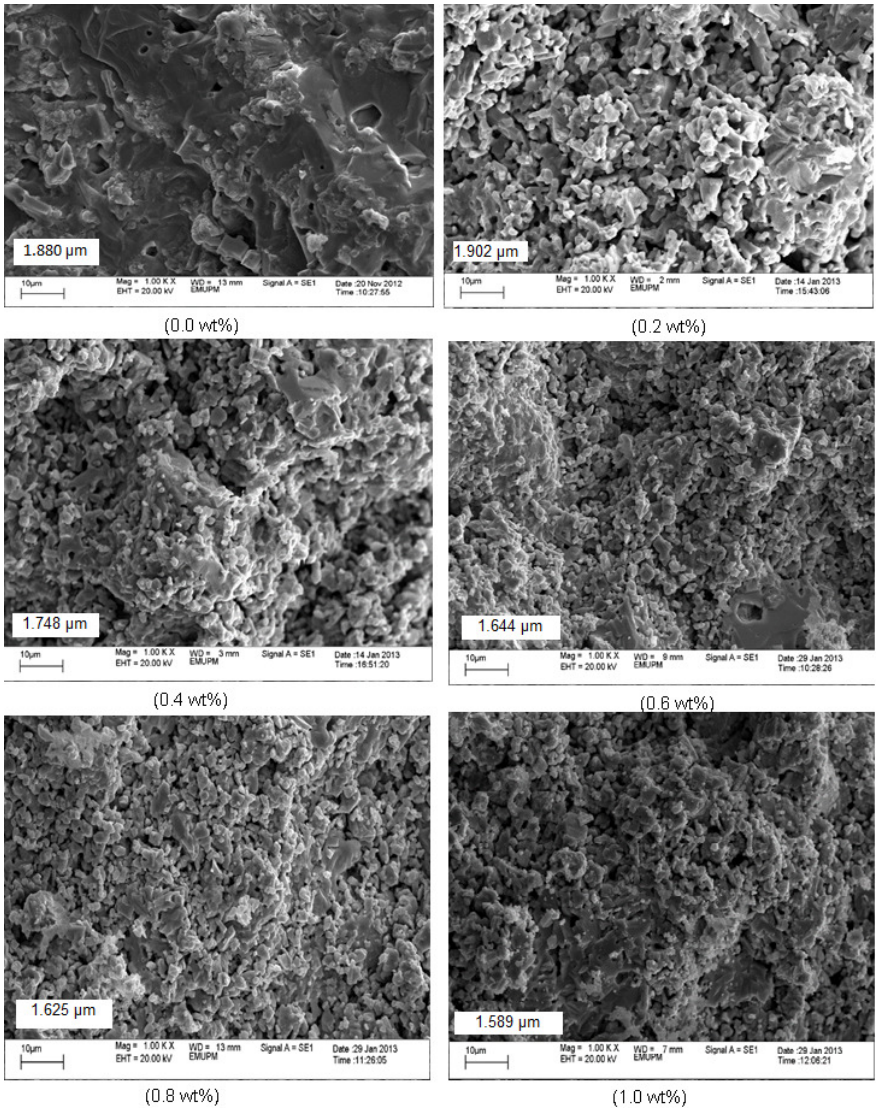

Figure 4. SEM images with average grain size measured from Image J for fractured YBCO + xSm_2O_3, x = 0.0, 0.2, 0.4, 0.6, 0.8 and 1.0 wt%.

In addition, the reduction of T_c and increasing of ΔT_c also might be due to the lowering of oxy-

gen content in samples. The results obtain from DC resistivity measurements are listed in Table 2.

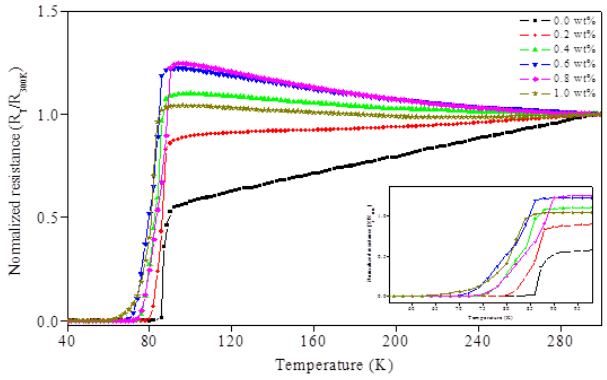

Figure 5. Normalized critical temperature, T_c for samples sintered with various amount of Sm_2O_3.

Table 2. The $T_{c-onset}$, $T_{c-offset}$, and transition width, ΔT_c for YBCO added with various amounts of Sm_2O_3.

Sm_2O_3, x	$T_{c-onset}$(K) ±	$T_{c-offset}$(K) ±	ΔT_c(K) ±
0.0	92	88	4
0.2	91	80	9
0.4	90	74	16
0.6	90	72	18
0.8	89	74	15
1.0	88	66	22

IV. SUMMARY

The $YBa_2Cu_3O_{7-\delta}$ superconductor added with Sm_2O_3 nanoparticle have been synthesised successfully by co-precipitation method. From the refinement of x-ray diffraction (XRD) data, it was found that the minor secondary phase, Y-211 and unreacted Sm_2O_3 have been observed for x = 0.2 1.0 wt% samples. The scanning electron microscope (SEM) showed that the samples decreased as the addition of Sm_2O_3 increased due to the non-homogenous distribution of Sm_2O_3 in structure and poor grain connectivity. The addition of Sm_2O_3 might cause the lowering of oxygen content in samples which resulted in reduction of critical temperature, $T_c$from 92 K to 88 K.

V. ACKNOWLEDGMENT

The authors would like to express gratitude to the Advanced Nano Materials (ANoMa) Research Group, School of Fundamental Science, Universiti Malaysia Terengganu and Superconductivity and Thin Film Laboratory, Department of Physics, Universiti Putra Malaysia for supporting this research project.

[1] Bednorz, J,G, Mller, K,A, 1986, Possible high T_c superconductivity in the Ba-La-Cu-O system, Condensed Matter, vol. 64, pp. 189 193.

[2] Wu, M,K, Ashburn, J,R, Torng, C,J, Hor, P,H, Meng, R,L, Gao, L, Huang, Z,J, Wang, Y,Q,

Chu, C,W, 1987, Superconductivity at 93 K in a new mixed-phase Y-Ba-Cu-O compound system at ambient pressure, *Physical Review Letters*, vol. 58 (9), pp. 908-910.

[3] Haugan, T, Barnes, P,N, Wheeler, R Meisenkothen, F, Sumption, M, 2004, Addition of nanoparticle dispersions to enhance flux pinning of the $YBa_2Cu_3O_{7-x}$, superconductor, *Nature*, vol. 430, pp. 867.

[4] Padam, G,K, Raman, V, Dhingra, I, Tripathi, R, Rao, S,U,M, Suri, D,K, Nagpal, K,C, Das, B,K, 1991, Synthesis and characterization of Y-Ba-Cu-O and Bi(Pb)-Sr-Ca-Cu-O superconductors from the oxine co-precipitation method, *Journal Physics Condensed Matter*, vol 3, pp. 4269-4279.

[5] Bahqiah, H, Halim, S,A, Chen, S,K, Lim, K,P, Awang Kechik, 2016, Effects of Rare Earth Nanoparticles (M = Sm_2O_2, Ho_2O_3, Nd_2O_3) Addition on the Microstructure and Superconducting Transition of $Bi_{1.6}Pb_{0.4}Sr_3Ca_2Cu_3O_{10+\delta}$, *Sains Malaysiana*, vol. 45(6), pp. 643-651.

[6] Jorgensen, J,D, Veal, B,W, Paulikas, A,P, Nowicki, G,W, Claus, H, Kwok, W,K, 1990, Structural properties of oxygen-deficient $YYBa_2Cu_3O_{7-\delta}$, *Physical Review B*, vol. 41(4), pp. 1863-1877.

[7] Mellekh, A, Zouaoui, M, Ben Azzouz, F, Annabi, M, Ben Salem, M, 2006, Nano-Al_2O_3 particle addition effects on $YBa_2Cu_3O_y$ superconducting properties, *Solid State Communications*, vol. 140, pp. 318-323.

[8] Moutalbi, N, Ouerghi, A, Djurado, E, Noudem, J G and Mchirgui, A, 2011, Vortex pinning in bulk-processed Y-Ba-Cu-O with ZrO_2 nanoparticles: Optimum pinning center size, *Physica C*, vol. 471, pp. 97-103.

[9] Mellekh, A, Zouaoui, M, Ben Azzouz, F, Annabi, M, Ben Salem, M, 2007, Effect of nanometer Al_2O_3 addition on structural and transport properties of $YYBa_2Cu_3O_{7-\delta}$, *Physica C*, vol. 460, pp. 426-427.

[10] Wahid, M,H, Zainal, Z, Hamadneh, I, Tan, K,B, Halim, S,A, Rosli, A,M, Alaghbari, E,S, Nazarudin, M,F and Kadri, E,F 2012, Phase formation of $REBa_2Cu_2O_{7-\delta}$ (RE : $Y_{0.5}Gd_{0.5}$, $Y_{0.5}Nd_{0.5}$, $Nd_{0.5}.5Gd_{0.5}$) superconductors from nanopowders synthesised via co-precipitation, *Ceramics International*, vol. 38, pp. 1187-1193.

[11] Bolzan, A,A, Millar, G,J., Bhargava, A, Mackinnon, I,D,R, Fredericks, P,M, 1996, A spectroscopic comparison of YBCO superconductors synthesised by solid-state and co-precipitation methods, *Materials Letters*, vol. 28, pp. 27-32.

[12] Veal, B,W, Paulikas, A,P, Downey, J,W, Claus, H, Vandervoort, K, Tomlins, G, Shi, H, Jensen, M, Morss, L, 1989, Varied oxygen stoichiometry in $RBa_2Cu_3O_{7-x}$, *Physica C* vol. 162, pp. 97-98.

[13] Aima, R, Halim, S,A, Baqiah, H, Chen, S,K, Wang Kechik, M,M, Talib, Z,A, 2016, Role of Nd_2O_3 nanoparticles addition on microstructural and superconducting properties of $YBa_2Cu_3O_{7-\delta}$ ceramics, *Journal of Rare Earths*, vol. 34 (9), pp. 895-900

[14] Ben Salem, M,K, Hannachi, E, Slimani, Y, Hamrita, A, Zouaoui, M, Bessais, L, Ben Salem, M, Ben Azzouz, F, 2014, SiO_2 nanoparticles addition effect on microstructure and pinning properties in $YBa_2Cu_3O_y$.*Ceramics International* , vol. 40, pp 4953-4962

[15] Dadras, S, Gharehgazloo, Z, 2016, Effect of Au nano-particles doping on polycrystalline YBCO high temperature superconductor, *Physica B*,

vol. 492, pp. 45-49.